Reprinted from

MATERIALS SCIENCE AND TECHNOLOGY

The Institute of Materials

Materials Science and Technology is published monthly and covers the science, fabrication, and engineering use of metals, ceramics, cements and concrete, polymers, composites, adhesives, and electronic materials.

Major themes are structure, physical and chemical properties, structure–property relationships, materials design, selection, and processing, service performance, and the development of new materials. The journal records scientific and technical advances, practical experience, and future trends in the science and technology of materials and in the design and development of related processes and plant.

Papers for submission should be sent to:
The Editor
Materials Science and Technology
The Institute of Materials
1 Carlton House Terrace
London SW1Y 5DB, UK

Subscription information may be obtained by writing to:
The Institute of Materials
Sales and Marketing Department
1 Carlton House Terrace
London SW1Y 5DB, UK

Texture and microstructure of rolled and annealed tantalum

D. Raabe, G. Schlenkert, H. Weisshaupt, and K. Lücke

Pure Ta has been cold rolled and annealed at various temperatures. The crystallographic textures were studied by measuring X-ray pole figures and subsequently calculating the orientation distribution function. The microstructure was investigated via optical microscopy. The rolling textures were explained by dislocation glide on {110}⟨111⟩, {112}⟨111⟩, and {123}⟨111⟩ glide systems. Corresponding simulations were carried out using relaxed constraints Taylor theory. Interpretation of the annealing textures was carried out via continuous recrystallisation in the case of weak deformations and temperatures and via discontinuous recrystallisation for higher rolling degrees and temperatures, respectively. MST/1886

 Manuscript received 19 April 1993; in final form 1 June 1993. *Dr Raabe and Professor Lücke are at the Institut für Metallkunde and Metallphysik, RWTH Aachen, Kopernikusstr., Aachen, Germany, and Dipl-Ing Schlenkert and Dipl-Phys Weisshaupt are with Rheinmetall GmbH, Düsseldorf, Germany.*

Introduction

Tantalum is a bcc transition metal with a melting point of 3000°C. Its investigation is of interest mainly for two reasons. First Ta is suitable for the examination of basic aspects of deformation, recovery, and recrystallisation of bcc metals over a wide temperature range, since it does not undergo phase transformation during annealing. Secondly Ta is of industrial importance due to its high melting point, low vapour pressure, good thermal and electrical conductivity, and biocompatibility.

Quantitative texture analysis and metallography represent a very sensitive tool for the investigation of rolled and annealed polycrystalline Ta, since the corresponding physical mechanisms, i.e. dislocation glide and recrystallisation, lead to characteristic changes of the orientation distribution of the crystallites.

Material and experimental procedure

The initial sheet of the electron beam melted, pure Ta (Table 1) had a thickness of 6 mm. Cold rolling was carried out on a laboratory rolling mill with a roll diameter of 250 mm. The specimen was cold rolled under oil lubrication in a strictly reversing manner, i.e. it was rotated 180° about the transverse direction after each pass.

Homogeneous rolling deformation is dependent on the ratio of the contact length between the sheet and the roll l_d and the thickness of the sheet d. The contact length can be estimated as $l_d \approx (r\Delta d)^{1/2}$ where Δd is the deformation per pass and r is the radius of the roll. Thus homogeneous deformation was carried out using a pass sequence obeying $1 < l_d/d < 3$ (Ref. 1). Samples for metallography and texture measurement were prepared after a deformation of $\varepsilon = 70$, 80, 90, and 95%.

A subsequent heat treatment was executed under vacuum at 1000, 1100, 1200, and 1300°C, respectively. Optical microscopy of longitudinal sections was carried out after etching in a solution of 100 ml H_2O, 80 ml HF, and 50 ml HNO_3 for 500 s at ambient temperature.

Table 1 Chemical analysis of Ta in 10^{-6} g/g

Nb	Mo	Fe	Ni	Si	W	Ti	Σ C, N, H, N
35	<2	<2	<3	<2	21	<21	<50

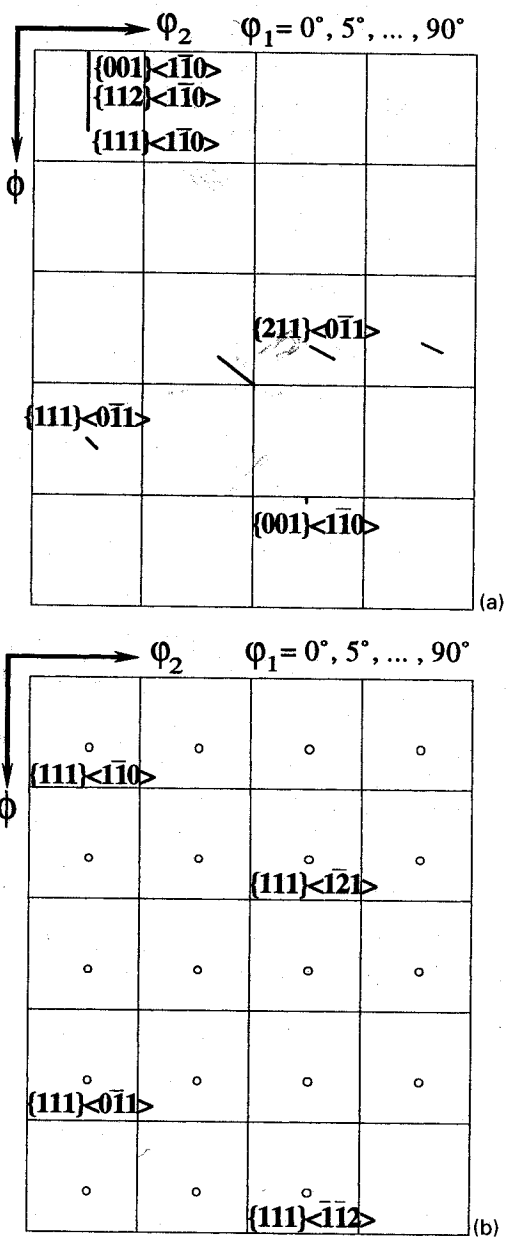

a α fibre; *b* γ fibre

1 Schematic diagrams showing α fibre and γ fibre in φ_1 sections

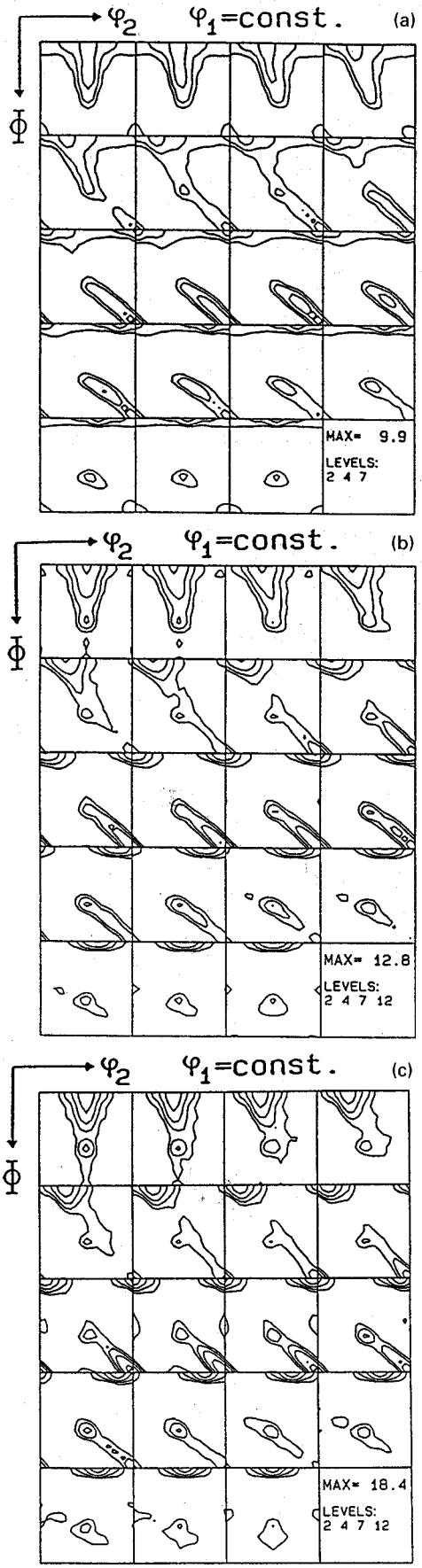

a 70% rolled; *b* 70% rolled + 1 h at 1000°C; *c* 70% rolled + 1 h at 1100°C

2 Rolling and annealing textures in φ_1 sections after cold rolling

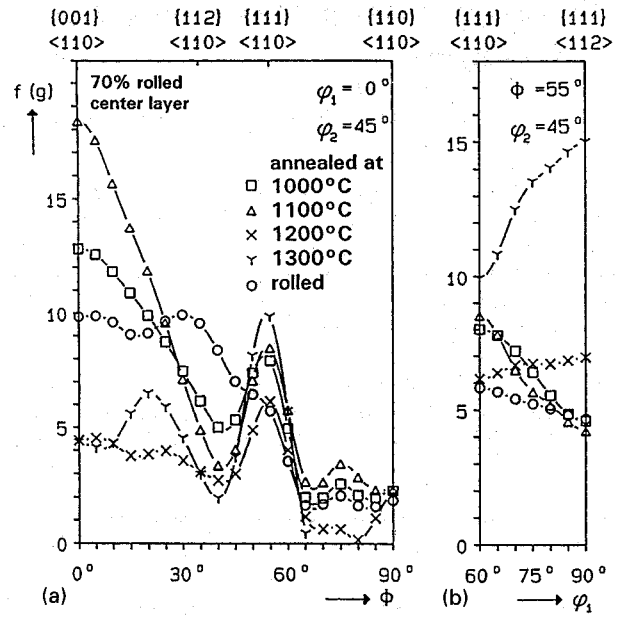

a α fibre; *b* γ fibre

3 Texture of 70% rolled specimens after various heat treatments

Measurement and description of textures

The textures were examined by measuring the four incomplete pole figures {110}, {200}, {112}, and {103} in the centre layer of the samples. The measurements were carried out in the range of the pole distance angle from 5 to 85° in the back reflection mode[2] using Mo $K\alpha_1$ radiation.

Since the pole figures taken from polycrystals represent two dimensional projections of the three dimensional texture, its interpretation is ambiguous because of the superposition of the poles. Therefore the orientation distribution function (ODF) was calculated using the series expansion method ($l_{max} = 22$).[3] For cubic crystal symmetry and orthorhombic sample symmetry, i.e. rolling, normal, and transverse directions (RD, ND, and TD) an orientation can then be defined by the three Euler angles φ_1, Φ, and φ_2 in the Euler space.[3] For better distinctness an orientation is often characterised by the Miller notation $\{hkl\}\langle uvw\rangle$. The first indices $\{hkl\}$ describe the crystallographic plane parallel to the sheet surface whereas the second indices $\langle uvw\rangle$ indicates the direction parallel to the RD.

As a rule, bcc metals reveal fibre textures after rolling and recrystallisation, respectively.[4,5] It is thus convenient to present the orientation distribution via isointensity diagrams in φ_1 sections through the Euler space or using fibre diagrams. In the first case the Euler space is cut along the φ_1 axis in 5° steps. In every φ_1 section the ODF is then presented by means of isointensity lines versus φ_2 and Φ (Fig. 1). In the second case the intensity of the orientations is depicted against the φ_1 or Φ angle respectively, while the other two coordinates remain constant.

Results

TEXTURES

The texture of the 70% rolled Ta reveals an incomplete α fibre, extending from $\{001\}\langle 110\rangle$ to $\{111\}\langle 110\rangle$, and a weaker γ fibre (Fig. 2*a*). After annealing at 1000°C for 1 h the $\{001\}\langle 110\rangle$ and the $\{111\}\langle 110\rangle$ orientation are

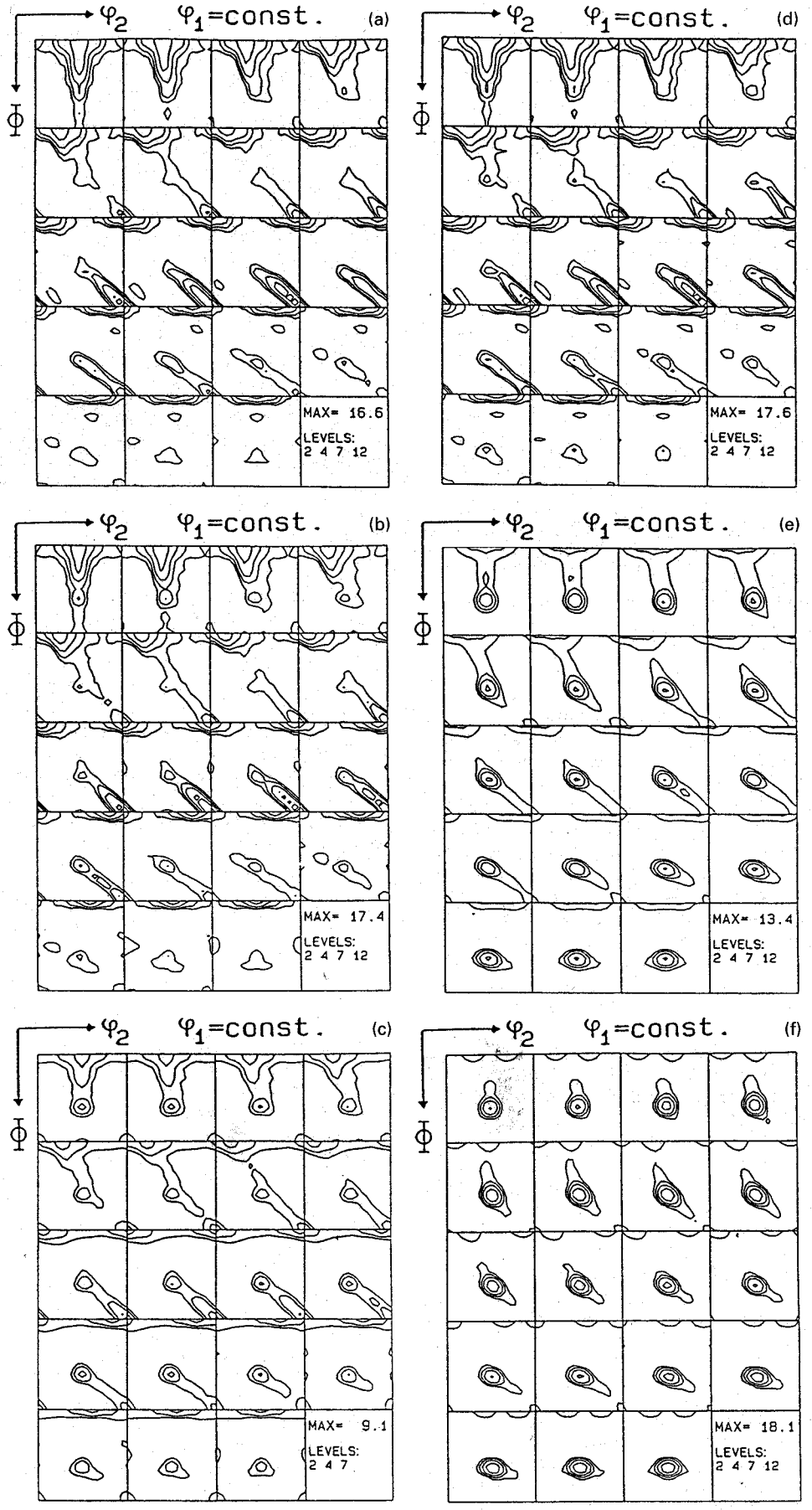

a 80% rolled; *b* 80% rolled + 1 h at 1000°C; *c* 80% rolled + 1 h at 1100°C; *d* 90% rolled; *e* 90% rolled + 1 h at 1000°C; *f* 90% rolled + 1 h at 1100°C

4 Rolling and annealing textures in φ_1 sections after cold rolling

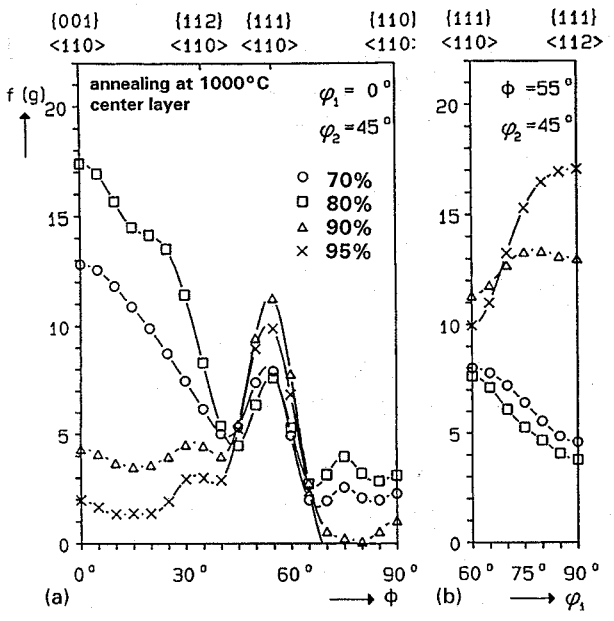

a α fibre; *b* γ fibre

5 Annealing textures for various rolling degrees after 1 h at 1000°C

sharpened whereas the {112}⟨110⟩ component is decreased (Figs. 2*b* and 3*a*). After annealing at 1100°C a similar tendency is revealed. The {001}⟨110⟩ orientation now reaches nearly twice the intensity than in the corresponding rolling texture (Figs. 2*a*, 2*c*, and 3*a*). After heat treatment at 1200 and 1300°C respectively, a change of the texture development is observed (Fig. 3). The intensity of the α fibre is reduced and the γ fibre exhibits a maximum at {111}⟨112⟩.

The texture after 80% rolling (Fig. 4*a*) corresponds to that of the 70% rolled specimen (Fig. 2*a*), although the α fibre has become stronger and the γ fibre weaker. The heat treatment leads mainly to the same texture changes as revealed for the 70% rolled sample. After annealing at 1000°C the α fibre is only sharpened at {001}⟨110⟩ and {111}⟨110⟩. The intermediate part of the fibre, i.e. the {112}⟨110⟩ component is decreased (Fig. 4*b*). After annealing at 1100°C, the {001}⟨110⟩ is also weakened whereas the orientations on the γ fibre become stronger (Fig. 4*c*).

After 90% rolling (Fig. 4*d*) the α fibre has become sharper than for lower rolling degrees. Annealing at 1000°C (Fig. 4*e*) and 1100°C (Fig. 4*f*) leads to a texture change. The orientations on the α fibre have vanished, especially after 1100°C and the γ fibre is enhanced.

In the fibre diagrams it can be observed that the type of annealing texture is dependent on the preceding degree of deformation (Fig. 5). For 70 and 80% deformation the {001}⟨110⟩ orientation becomes the strongest component (Fig. 5*a*) whereas for 90 and 95% a decrease of the α fibre and a strong increase of the γ fibre, especially of {111}⟨112⟩ is revealed (Fig. 5*b*). Higher temperatures lead to the formation of the γ fibre even after lower rolling degrees (Figs. 2*c* and 4*c*).

MICROSTRUCTURE

The longitudinal micrographs of the rolled samples expose a flat and elongated grain morphology (Figs. 6*a* and 6*d*). After annealing at 1000°C, the microstructure appears inhomogeneous especially for the 70% rolled sample (Fig. 6*b*). Whereas in some regions new grains are formed, adjacent zones exhibit residual deformation structure. The 90% rolled sample reveals nearly complete reformation of the microstructure after annealing at 1000°C (Fig. 6*e*). In both samples the new grains often have an elongated instead of an equiaxed shape. A low preceding rolling degree leads to a high amount of residual deformation structure. After annealing at 1100°C the grain morphology is entirely rearranged in all samples (Figs. 6*c* and 6*f*). Only the 70% rolled specimen reveals some tiny areas with residual deformation structure. It should be noted that, although in both depicted samples, i.e. 70 and 90% rolled, the initial deformation microstructure has been removed during annealing at 1100°C (Figs. 6*c* and 6*f*) the textures of both specimens are completely different (Figs. 2*c* and 4*f*). This indicates that different mechanisms were involved in the reformation of the microstructure during annealing.

Discussion

ROLLING TEXTURES

The evolution of the rolling texture can be understood in terms of the relaxed constraints Taylor theory.[6] Simulations of the rolling texture according to Taylor[7] are based on the accomplishment of macroscopic deformation by means of crystallographic slip. Macroscopic deformation is described by the displacement gradient tensor. Whereas its symmetric part represents the strain tensor, its antisymmetric part characterises the resulting lattice rotation. The macroscopic deformation during rolling consists of elongation in RD and thickness reduction parallel to the ND, but no shears are involved.

The relaxed constraints Taylor theory also assumes shear strains to occur microscopically between adjacent grains, i.e. relaxes the zero shear constraints locally. A relaxation of the strain component ε_{13} corresponds to a shear in RD, whereas ε_{23} denotes the shear in TD (Fig. 7). Allowing for these shears locally leads to distinct changes in the selection of the active glide systems in the resulting rigid body rotation, and thus in the texture development when compared with the predictions of the full constraints Taylor theory.[7]

In the simulations presented here two specific assumptions were made. First, the ε_{13} and the ε_{23} tensor components were both relaxed since fairly high deformation degrees were investigated. It was thus assumed that the pancakelike shape of the grains admits local shears in RD and TD (Fig. 7). Secondly, dislocation glide on {110} planes (Fig. 8*a*), {110} and {112} planes (Fig. 8*b*), and {110}, {112}, and {123} planes (Fig. 8*c*) was considered.[8–10]

The simulation on the basis of the 12 {110} glide systems (Fig. 8*a*) leads to a texture which is dominated by the two isolated orientations {112}⟨110⟩ and {111}⟨110⟩. The fibre texture of the rolled Ta (Figs. 2*a*, 4*a*, and 4*d*) stretching from {001}⟨110⟩ to {111}⟨110⟩ is not adequately simulated. Considering also the 12 {112} glide systems (Fig. 8*b*) yields two main orientations {001}⟨110⟩ and {111}⟨110⟩. Although the simulated texture has changed to a more fibrelike shape when compared with Fig. 8*a*, the contour of the measured α fibre is not convincingly reproduced.

Taking into account additionally the 24 {123} glide systems (Fig. 8*c*) the simulations show a uniformly shaped α fibre, i.e. in good accordance with the measurements. The introduction of different critical shear stresses for the three types of glide system did not yield more favourable results. It follows therefore that during rolling of pure Ta at ambient temperatures, dislocation glide on {110}, {112}, and {123} planes takes place and that the corresponding critical shear stresses are similar to one another.

ANNEALING TEXTURES

The annealing of rolled Ta basically generated two types of texture: first the enhancement of {001}⟨110⟩

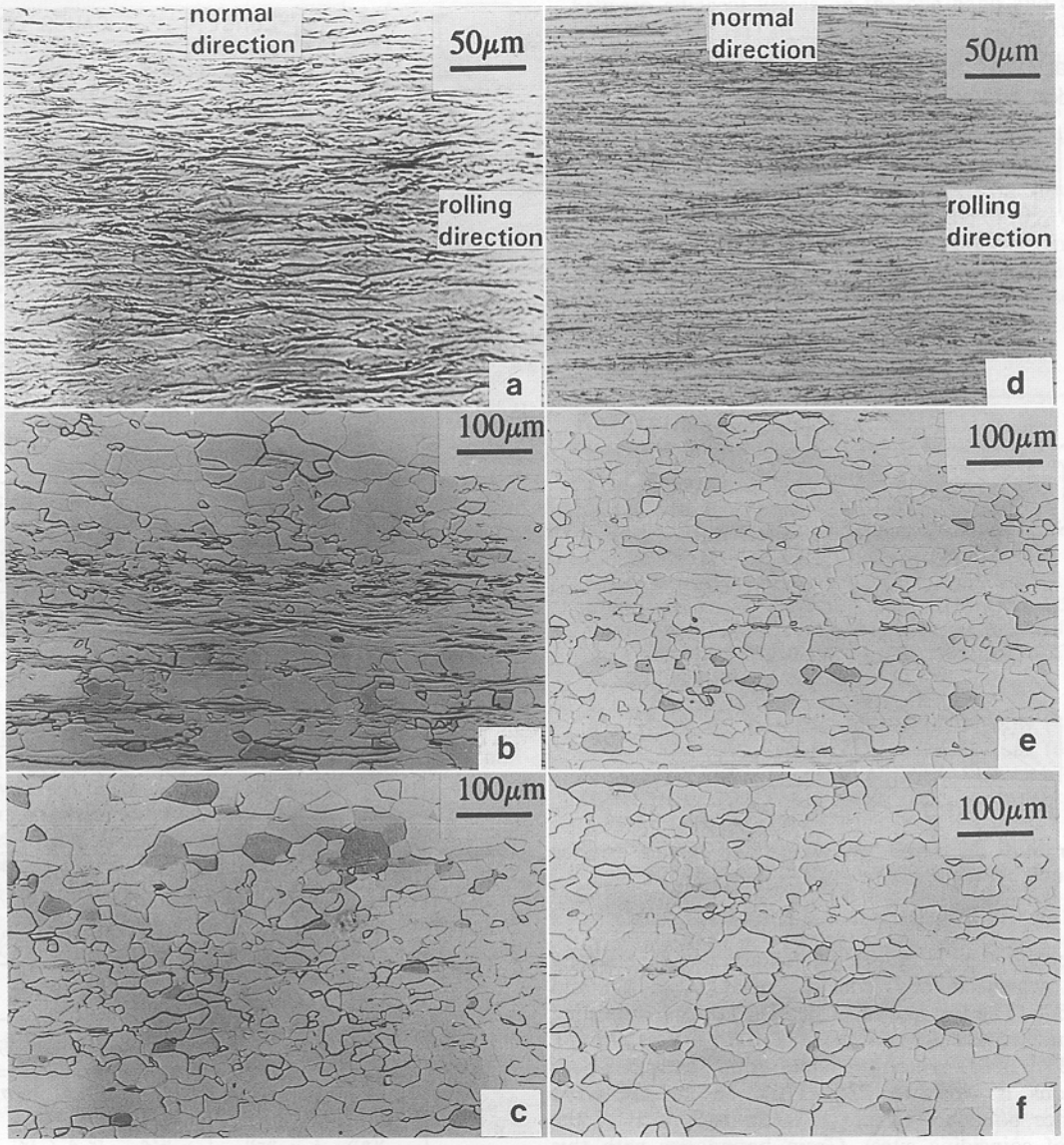

a 70% rolled; *b* 70% rolled + 1 h at 1000°C; *c* 70% rolled + 1 h at 1100°C; *d* 90% rolled; *e* 90% rolled + 1 h at 1000°C; *f* 90% rolled + 1 h at 1100°C

6 Longitudinal micrographs of samples after cold rolling

accompanied by the decrease of {112}⟨110⟩ for moderate deformations and temperatures (70%/1000°C, 1100°C and 80%/1000°C as shown in Figs. 3 and 5); and secondly the strong decrease of the α fibre between {001}⟨110⟩ and {112}⟨110⟩ accompanied by the sharp increase of the γ fibre for higher deformations and temperatures (Figs. 3, 4*e*, 4*f*, and 5).

As has been noted by various authors,[11,12] the stored dislocation energy and the dislocation arrangement, which represent the driving force and the nucleation sites for primary recrystallisation respectively, depends on the orientation of the deformed grain. Dillamore *et al.* showed that the size of subgrains and the average misorientation across the subgrain boundaries in deformed polycrystalline iron reveals a clear dependence on the orientation of the grain.[11,13] Whereas the subgrain size decreases with increasing Φ angle on the α fibre, the misorientation between adjacent cells is enhanced. Dillamore and co-workers also elucidated how this variation of stored energy at a given strain in rolled iron correlated with a variation of the Taylor factor.[13,14] The Taylor factor is a calculated value which represents the sum of the glide steps on the selected glide systems which are necessary to achieve compatible deformation of a certain grain, divided by the chosen deformation interval.

The {001}⟨110⟩ orientation reveals a very low Taylor factor (Fig. 9) i.e. a low dislocation density.[11,14] Also line broadening experiments have shown that the dislocation density in {001}⟨*uvw*⟩ is smaller than in {112}⟨*uvw*⟩ or {111}⟨*uvw*⟩.[15] It is thus assumed that the {001}⟨110⟩ oriented grains reveal a low stored energy and hence a weak tendency to form nuclei during recrystallisation. This reluctance of {001}⟨110⟩ to recrystallisation was also observed in pure Fe by applying single orientation measurements.[16]

Since {001}⟨110⟩ grains are not able to form nuclei, the enhancement of {001}⟨110⟩ during annealing (Figs. 2*b*, 2*c*, and 3*a*) cannot be explained by recrystallisation. However, this texture also cannot be understood in terms of recovery. First the measured increase of {001}⟨110⟩ is much stronger than would be caused merely by the decrease of diffuse scattering. Secondly the microstructure, especially of the 70% rolled and annealed samples, reveals a partial (Fig. 6*b*) or even complete (Fig. 6*c*) reformation of the grain morphology. Since no texture transition has taken place, i.e. {001}⟨110⟩ has only increased during annealing, and since new grains have been formed without preceding nucleation and thus without movement of large angle grain boundaries, the observed texture is attributed to continuous recrystallisation, i.e. recrystallisation *in situ*.

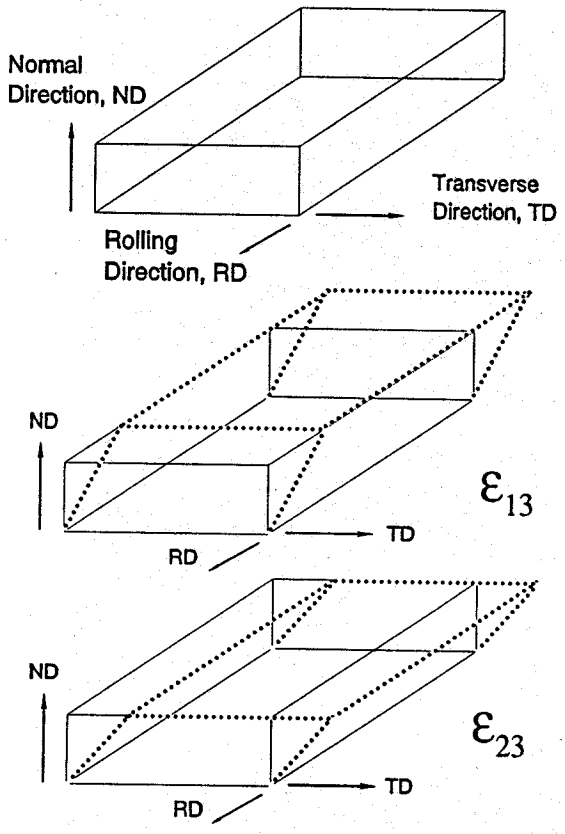

7 Schematic diagrams showing two shear modes between adjacent grains

The second type of annealing texture reveals a strong γ fibre, which mainly consists of {111}⟨110⟩ and {111}⟨112⟩. The increase of {111}⟨112⟩ during annealing corresponds to the decrease of {112}⟨110⟩ (Figs. 4*e*, 4*f*). The ~35° ⟨110⟩ rotation relationship between both orientations is close to 27° ⟨110⟩, i.e. to the Σ19a coincidence boundary (where Σ is the reciprocal of the density of coinciding sites). Grain boundaries with this rotation relationship are known to reveal high growth rates.[17] It is therefore assumed that growth selection plays the leading role in the development of the {111}⟨112⟩ recrystallisation component. This is also valid for the {111}⟨110⟩ recrystallisation orientation, which has a good growth relationship with the {113}⟨110⟩ rolling component (Figs. 4*d*–4*f*). On the other hand it reveals a very fine cell structure[8–10] and a high Taylor factor (Fig. 9) exceeding even that of {111}⟨112⟩. This indicates a high nucleation tendency. It is thus assumed that the occurrence of a strong {111}⟨110⟩ recrystallisation component results from both a high nucleation rate and growth selection.

COMPARISON BETWEEN Ta AND FERRITIC STEELS

The texture development of bcc metals has been widely investigated using pole figures concentrating mainly on ferritic steels (e.g. Refs. 11–14). In the last decade however the resolution of texture investigation has been remarkably enhanced owing to the introduction of the ODF.[3] In the measurements presented above various results correspond to similar findings received from Fe and ferritic steels,[16,18–20] although phase transformation does not allow the investigation of annealing textures over a wider temperature range for these materials.

The rolling textures of Ta and Fe can both be understood by means of relaxed constraints Taylor theory taking into account relaxation of either ε_{13} or ε_{13} and ε_{23} on the one

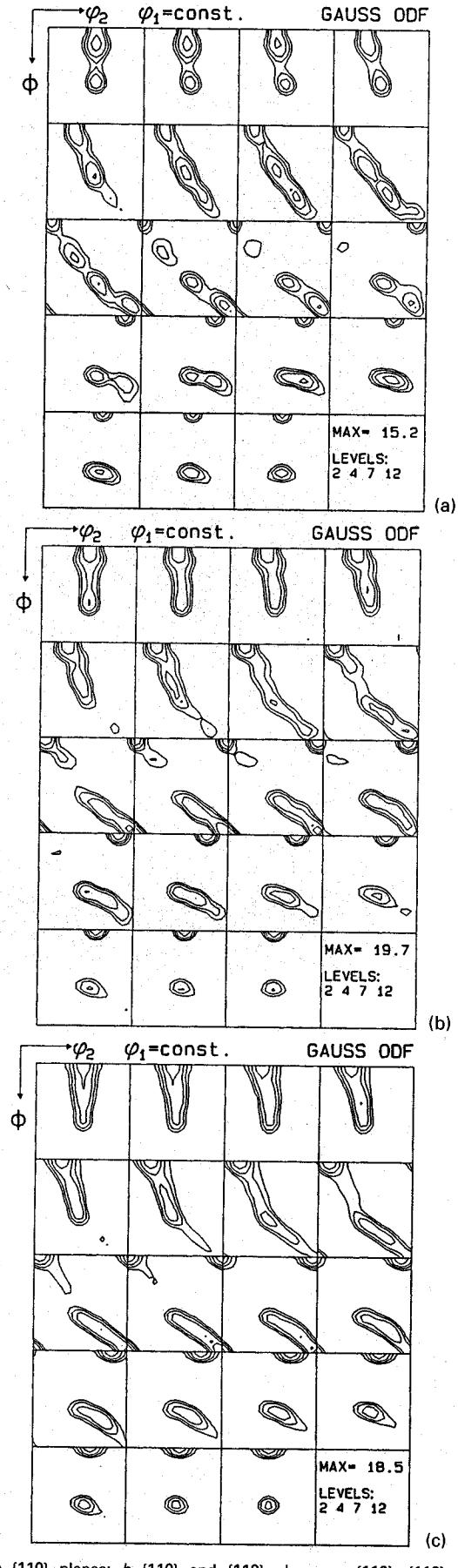

a {110} planes; *b* {110} and {112} planes; *c* {110}, {112}, and {123} planes

8 Simulations according to relaxed constraints Taylor theory for 70% deformation and relaxation of ε_{13} and ε_{23}: dislocation glide on various planes, φ_1 sections

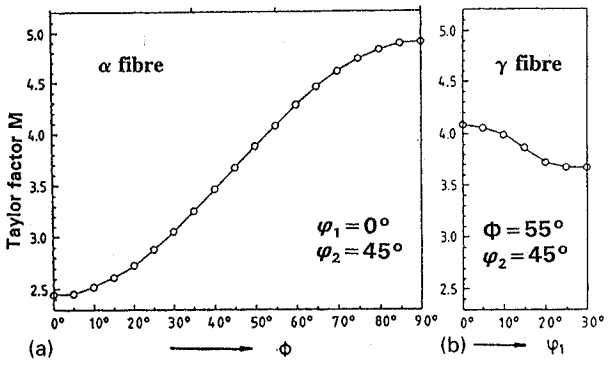

a α fibre; *b* γ fibre

9 Calculated Taylor factors for bcc crystals under plain strain deformation

hand and activation of dislocation glide on {110}, {112}, and {123} glide planes on the other hand. The recrystallisation texture of Fe which is typically dominated by a strong γ fibre was also found for Ta in the case of strong deformation and high annealing temperatures. However, the main difference in the textures between both materials is the strong continuous recrystallisation, which was found for the 70% rolled and annealed Ta. The reason for this difference could be the high purity of the Ta used in the present work which generally allows an increased non-conservative mobility of the dislocations and hence strong recovery or even continuous recrystallisation. On the other hand microstructural inhomogeneities such as microbands, shear bands, or divergent zones which often occur as nucleation sites in steels, were not found in Ta. Thus a lack of potential nucleation sites could also be a reason for the continuous recrystallisation of Ta.

Conclusions

1. Rolling textures of polycrystalline Ta can be interpreted by means of relaxed constraints Taylor theory. The simulations which take into account ε_{13} and ε_{23} shear between adjacent grains on the one hand and dislocation glide on {110}, {112}, and {123} planes on the other hand, yield satisfying correspondence with the measured rolling textures.

2. Specimens with rolling degrees up to 80% which are annealed below 1200°C reveal an inhomogeneous development of the texture and microstructure. Whereas the rolling component {112}⟨110⟩ is consumed via discontinuous recrystallisation grains with a {001}⟨110⟩ orientation are rearranged by continuous recrystallisation. In specimens with stronger deformation and/or higher annealing temperature a strong γ fibre texture is formed by discontinuous recrystallisation.

References

1. W. TRUSZKOWSKI, J. KROL, and B. MAJOR: *Metall. Trans.*, 1980, **11A**, 749.
2. L. G. SCHULZ: *J. Appl. Phys.*, 1949, **20**, 1030.
3. H. J. BUNGE: *Z. Metallkd.*, 1965, **56**, 872.
4. I. L. DILLAMORE and W. T. ROBERTS: *Acta Metall.*, 1964, **12**, 281.
5. I. L. DILLAMORE: *Trans. Met. Soc. AIME*, 1965, **233**, 702.
6. H. HONNEFF and H. MECKING: in Proc. 6th Int. Conf. on 'Texture of Materials', (ICOTOM 6), 347; 1981, Tokyo, The Iron and Steel Institute of Japan.
7. G. I. TAYLOR: *J. Inst. Met.*, 1938, **62**, 307.
8. B. SESTÁK and A. SEEGER: *Z. Metallkd.*, 1978, **69**, (4), 195.
9. B. SESTÁK and A. SEEGER: *Z. Metallkd.*, 1978, **69**, (6), 355.
10. B. SESTÁK and A. SEEGER: *Z. Metallkd.*, 1978, **69**, (7), 425.
11. I. L. DILLAMORE, C. J. E. SMITH, and T. W. WATSON: *Met. Sci. J.*, 1967, **1**, 49.
12. W. B. HUTCHINSON: *Int. Mater. Rev.*, 1984, **29**, 25.
13. I. L. DILLAMORE, P. L. MORRIS, C. J. E. SMITH, and W. B. HUTCHINSON: *Proc. R. Soc.*, 1972, **A329**, 405.
14. I. L. DILLAMORE and H. KATOH: *Met. Sci.*, 1974, **8**, 21.
15. P. PARNIERE: in Proc. Int. Conf. on 'Texture of Materials', (ICOTOM 6), 181; 1981, Tokyo, The Iron and Steel Institute of Japan.
16. D. RAABE and K. LÜCKE: *Scr. Metall.*, 1992, **27**, 1533.
17. G. IBE and K. LÜCKE: *Arch. Eisenhüttenwes.*, 1968, **39**, (9), 693.
18. M. HÖLSCHER, D. RAABE, and K. LÜCKE: *Steel Res.*, 1991, **62**, 567.
19. R. KERN, H. P. LEE, and H. J. BUNGE: *Steel Res.*, 1986, **57**, 563.
20. K. USHIODA, W. B. HUTCHINSON, J. ÅGREN, and U. v. SCHLIPPENBACH: *Mater. Sci. Technol.*, 1986, **2**, (8), 807.